Selectivity of vacuum ammonia stripping using porous gas-permeable and dense pervaporation membranes under various hydraulic conditions and feed water compositions

van Linden, Niels; Wang, Yundan ; Sudhölter, Ernst ; Spanjers, Henri; van Lier, Jules B.

DOI
10.1016/j.memsci.2021.120005

Publication date
2022

Document Version
Final published version

Published in
Journal of Membrane Science

Journal of Membrane Science 642 (2022) 120005

Contents lists available at ScienceDirect

Journal of Membrane Science

journal homepage: www.elsevier.com/locate/memsci

Selectivity of vacuum ammonia stripping using porous gas-permeable and dense pervaporation membranes under various hydraulic conditions and feed water compositions

Niels van Linden [a,*], Yundan Wang [a], Ernst Sudhölter [b], Henri Spanjers [a], Jules B. van Lier [a]

[a] Delft University of Technology, Faculty of Civil Engineering and Geosciences, Stevinweg 1, 2628, CN, Delft, the Netherlands
[b] Delft University of Technology, Faculty of Applied Sciences, Van der Maasweg 9, 2629 HZ, Delft, the Netherlands

ARTICLE INFO

Keywords:
Ammonia
Water vapour
Stripping
Selectivity
Mass transfer coefficient
Pervaporation

ABSTRACT

Recovery of ammonia (NH_3) from residual waters offers various reuse opportunities, such as the production of fertilisers and the generation of electricity and heat. However, simultaneous evaporation of water (H_2O) during NH_3 stripping under vacuum results in diluted recovered NH_3 gas with high H_2O contents. Whereas porous gas-permeable membranes are already used for vacuum NH_3 stripping, the use of non-porous silica-based pervaporation (PV) membranes showed promising results in recent literature, with respect to more selective transfer of NH_3 compared to H_2O. In this study, we assessed the selectivity of NH_3 over H_2O transfer ($S_{NH3/H2O}$) for different types of membranes, under various hydraulic conditions and feed water compositions. The three following membranes were tested: a porous gas-permeable polytetrafluoroethylene (PTFE) membrane, a hydrophilic (Hybrid Silica PV) membrane and a hydrophobic polydimethylsiloxane PV (PDMS PV) membrane.

For the PTFE and the Hybrid Silica PV membrane, $S_{NH3/H2O}$ ranged between 0.1 and 0.4, indicating that the transfer of NH_3 was consistently less preferred compared to the transfer of H_2O. The preference for H_2O over NH_3 transfer through the membranes at various hydraulic conditions and feed water compositions can be assigned to the similarity in polarity and kinetic diameter of NH_3 and H_2O and the low relative concentration of NH_3 in the used feed waters (approximately 0.1–1.0 wt%). The PDMS PV membrane showed negligible NH_3 transfer and deteriorated rapidly during the NH_3 stripping experiments. The $S_{NH3/H2O}$ of both gas-permeable and PV membranes was higher for unsteady than for steady hydraulic conditions. Furthermore, the $S_{NH3/H2O}$ of the both PTFE and the Hybrid Silica decreased when the ionic strength of the feed water increased from 0.0 to 0.8 mol•L^{-1} and when the NH_3 feed water concentration increased from 1 to 10 g•L^{-1}. According to the results, the used PV membranes did not show selectivity of NH_3 over H_2O transfer. In fact, the used PV membranes consistently had a lower $S_{NH3/H2O}$ than the PTFE membrane. Hence, the dense silica-based PV membranes did not allow for the recovery of gaseous NH_3 from water, with lower H_2O content in the recovered gas, compared to porous PTFE membranes.

1. Introduction

1.1. Recovery and use of gaseous ammonia

In contrast to the application of conventional biochemical technologies to remove NH_3 from residual waters, recovery of NH_3 offers multiple opportunities for reuse [1]. Biochemical treatment for the removal of NH_3 from water, such as nitrification in combination with denitrification and/or partial nitritation in combination with anaerobic ammonium oxidation (anammox), relies on the biochemical conversion of NH_3 to nitrogen gas (N_2), which is an energy-consuming process, while strong greenhouse gases such as nitrous oxide (N_2O) are emitted [2]. Ammonia (NH_3) can be recovered from residual waters in the form of ammonium (NH_4^+) salt solutions or solid crystals, which can be used as (a resource for the production of) fertilisers [1]. Furthermore, according to the review study of Deng et al. [1], NH_3 can also be recovered for the production of microbial proteins or for the generation of energy in combustion-based or fuel cell technologies, opening new opportunities for NH_3 recovery and treatment methods of residual waters that contain NH_3.

* Corresponding author.
E-mail address: N.vanLinden@tudelft.nl (N. van Linden).

https://doi.org/10.1016/j.memsci.2021.120005
Received 25 July 2021; Received in revised form 2 October 2021; Accepted 20 October 2021
Available online 23 October 2021

1.2. Evaporation of water during recovery of gaseous ammonia from water

During NH_3 recovery by vacuum stripping processes, such as vacuum membrane stripping (VMS) using porous gas-permeable membranes, stripping of NH_3 is accompanied by the evaporation of H_2O, which dilutes the obtained gaseous NH_3 [3–5]. To obtain more concentrated NH_3 gas, the concentration of NH_3 in the feed water can be increased [5–7]. Moreover, according to our previous study, increasing the feed water temperature at an NH_3 feed concentration of 10 g•L^{-1} from 25 to 35 °C results in an increase in NH_3 concentration in the permeate from 8 to 11 wt%. However, a further increase in the feed water temperature to 45 and 55 °C leads to dilution of NH_3 in the gaseous permeate to 5 and 4 wt %, respectively [5]. To obtain more concentrated NH_3 by VMS, the evaporation of H_2O must be minimised. To this end, a physical barrier for the transfer of H_2O that does not negatively affect the NH_3 transfer may be introduced. Porous gas-permeable membranes are not considered to be effective barriers, because the pore size of about 0.1 μm is at least two orders of magnitude larger than the kinetic diameter of transferred molecules such as NH_3 and H_2O (<1 nm). To recover more concentrated NH_3 by vacuum stripping processes, the use of dense pervaporation (PV) membranes to more selectively transfer NH_3 through the membrane was initially proposed by Yang et al. [8].

1.3. Selectivity of ammonia transfer through PV membranes

For PV, selectivity (S) is defined as the ratio of the permeances of the respective gases permeating through the membrane, whereas the permeance describes the normalised transfer rate: the mass flux normalised for the driving force [9]. Hence, selectivity ($S_{i/j}$) describes the normalised transfer rate of gas 'i' with respect to another gas 'j'. In this view, selective transfer of 'i' over 'j' is considered when $S_{i/j} > 1$. Selective permeation of NH_3 over hydrogen (H_2) and N_2 by using PV membranes proved to be feasible for gas separation, for the recovery of NH_3 from gas mixtures consisting of the respective gases [10,11]: $S_{NH3/H2}$ and $S_{NH3/N2} > 1$. Camus et al. [10] showed that silica-based PV membranes had a seven and fourteen times higher NH_3 permeance compared to the permeance of H_2 and N_2 when using mixtures of NH_3–H_2 and NH_3–N_2 gas as a feed at a temperature of 80 °C. Subsequently, Kanezashi, et al. [11] reported H_2 permeances up to twenty times higher than the NH_3 permeances for silica-based PV membranes when pure H_2 and NH_3 gas were used as the feed at a temperature of 50 °C. However, when mixtures of NH_3/H_2 gas were used as feed at the same temperature, selective transfer of NH_3 over H_2 took place ($S_{NH3/H2}$ of 29), in agreement with Camus et al. [10]. Both Camus et al. [10] and Kanezashi et al. [11] attributed the selective transfer of NH_3 over H_2 to the adsorption of NH_3 to the membrane material, which contained silica groups. According to Kanezashi et al. [11], NH_3 and H_2 have a kinetic diameter of 0.33 and 0.26 nm, respectively. Hence, for pure gases, the transfer rate of H_2 is higher than the transfer rate of NH_3 based on the higher reported permeances, but when gaseous NH_3–H_2 mixtures are present in the feed, NH_3 adsorbs on the membrane interface and hinders the adsorption and permeation of H_2, resulting in selective transfer of NH_3 over H_2 [10,11].

1.4. Recovery of gaseous ammonia from feed waters using PV membranes

In addition to the application to obtain more enriched permeate streams from gas mixtures by gas separation, PV membranes can also be used to remove and/or recover gases from a liquid feed such as water. According to the review of Jyoti et al. [12], different types of PV membranes are used to allow for either selective transfer of water (H_2O) or volatile organics from liquid H_2O-organics mixtures. For the selective transfer of H_2O from liquid H_2O-organics mixtures, hydrophilic PV membranes are used, whereas hydrophobic PV membranes are used for selective transfer of volatile organics, such as alcohols or volatile fatty acids.

Research of Yang et al. [8] focused on the recovery of gaseous NH_3 from liquid feed water, using silica-based PV membranes that were hydrothermally-treated by addition of iron and cobalt in the membrane material. Yang et al. [8] did not report on the transfer selectivity of the PV membranes according to the proposed definition of Baker et al. [9], but did report concentration factors up to 63 for a PV membrane for an NH_3 feed concentration of 0.8 g•L^{-1} at feed temperatures ranging between 45 and 50 °C. Because the concentration factor represents the ratio of the NH_3 concentration in the permeate and the feed, the relatively high concentration factors suggest high transfer rates of NH_3 compared to H_2O. In a follow-up study, Yang, et al. [13] stripped NH_3 from liquid water using a PV membrane that contained a combination of silica and organic groups for hydrothermal stability in the selective layer and was further referred to as hybrid-silica. For an NH_3 feed concentration of 50 mg•L^{-1} and at a feed temperature of 45 °C, the authors reported a concentration factor of 12 and an $S_{NH3/H2O}$ of 0.5, indicating selective transfer of H_2O over NH_3 for the used PV membranes. Finally, Yang, et al. [14] assessed the effect of cobalt content in the selective layer of silica-based PV membranes on the transfer of H_2O and NH_3 and observed again selective transfer of H_2O over NH_3 ($S_{NH3/H2O} < 1$).

Hence, in currently available literature, there is no consensus on whether selective transfer of NH_3 over H_2O can be achieved by using silica-based PV membranes. The differences in transfer selectivity observed in previous studies may be explained by the differences in applied experimental conditions, as Yang et al. [8] and Yang et al. [14] used configurations in which the membranes were submerged in the feed water, whereas Yang et al. [13] used a cross-flow configuration. The mentioned studies did not describe the location of the selective layer on the membranes. The location of the selective layer of the membrane and the used configuration are key to control the hydraulic conditions, which affect polarisation effects at the membrane interface, which in their turn affect the mass transfer rates through the membrane [15]. Furthermore, the contradicting results on the transfer selectivity of NH_3 over H_2O also may be explained by differences in tested feed characteristics, such as feed temperature and NH_3 feed concentration.

1.5. Research objective

Currently available literature showed that silica-based PV membranes allow for selective transfer of NH_3 over N_2 and H_2 when treating gas mixtures, but it remains unclear whether also selective transfer of NH_3 over H_2O can be achieved when stripping NH_3 from liquid water. Silica-based PV membranes are considered to be hydrophilic, indicating that these membranes allow for the transfer of H_2O. To our best knowledge, it is unknown whether hydrophobic silica-based PV membranes allow for selective transfer of NH_3 when stripping NH_3 from water. Furthermore, according to available literature, there is no clarity whether PV membranes have higher $S_{NH3/H2O}$ compared to conventional porous gas-permeable membranes. Therefore, in this study, we assessed the mass transfer rates and $S_{NH3/H2O}$ of a porous gas-permeable membrane and dense hydrophilic and hydrophobic PV membranes while stripping NH_3 from water. We assessed the effect of the hydraulic conditions and the feed composition, in terms of NH_3 feed concentration and ionic strength, on the $S_{NH3/H2O}$ for the various membranes.

2. Materials and methods

2.1. Materials

For the porous gas-permeable membrane experiments, we used the same equipment and spacer-filled flat sheet membrane configuration as described in our previous study [16]. For the experiments with the PV membranes, again the same experimental set-up was used, except a stainless-steel membrane housing was used for the tubular PV membranes, including rubber rings at the ends of the PV membranes to ensure liquid and gas tightness. Fig. 1 presents the experimental set-up,

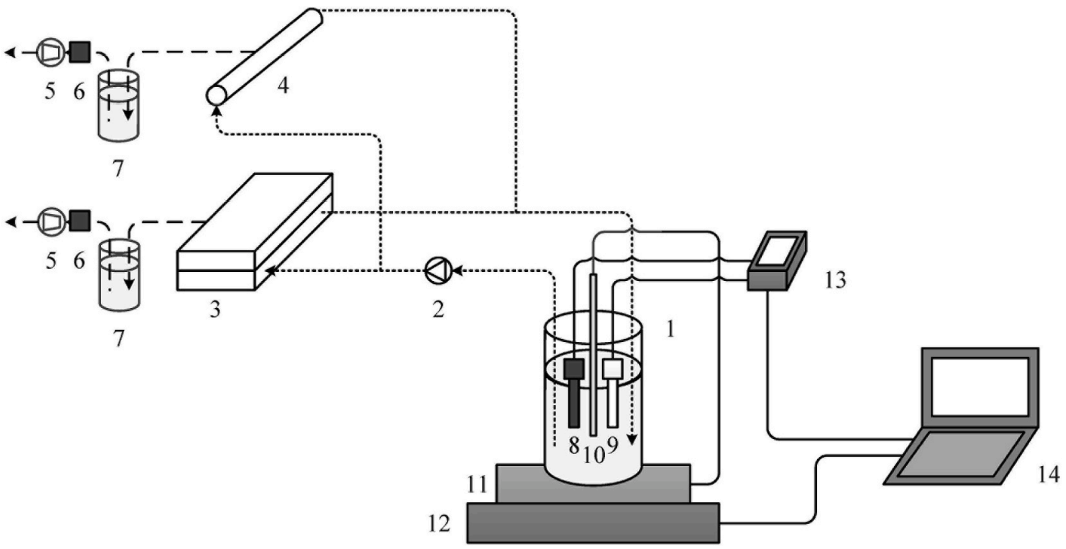

Fig. 1. Schematic representation of the used experimental set-up including feed water bottle (1), peristaltic pump (2), gas-permeable membrane housing including membrane (3), PV membrane housing including membrane (4), vacuum pump (5), pressure sensor (6), cooled permeate scrubber (7), EC-sensor (8), pH-sensor (9), temperature sensor (10), integrated heating and mixing plate (11), balance (12), multimeter (13) and laptop (14).

including the membrane housings for the porous gas-permeable and PV membranes. The porous gas-permeable membrane was a Sterlitech polytetrafluoroethylene membrane (hereafter PTFE membrane) and the PV membranes were a hydrophilic Pervatech Hybrid Silica (hereafter Hybrid Silica PV membrane) and a hydrophobic Pervatech polydimethylsiloxane membrane (hereafter PDMS PV membrane). Table 1 presents an overview of the specific characteristics and measured dimensions of the used membranes.

The feed waters were prepared by the addition of Acros Organics 25 wt% ammonium hydroxide (NH_4OH) stock solution, or Sigma Aldrich ammonium bicarbonate (NH_4HCO_3) salt and Merck 1 M sodium hydroxide (NaOH) solution to demineralised water. The used NH_4OH solution, NH_4HCO_3 salt and NaOH solution were all analytical grade. The prepared feed waters consisted of NH_4HCO_3 because bicarbonate (HCO_3^-) is often the main anion in nitrogen-rich residual streams, such as reject waters, urine and industrial condensates. All experimental runs were conducted in at least triplicate.

2.2. Performance indicators

For the assessment of the $S_{NH3/H2O}$, the overall mass transfer coefficient (K_o) for NH_3 and H_2O was determined. The K_o normalises the mass flux with respect to the respective driving force for the transfer of gases, which for NH_3 and H_2O is the vapour pressure difference between the liquid feed water and the gaseous permeate. K_o is usually described by a series-resistance model, consisting of three separate components: the mass transfer coefficients for the liquid feed water (K_f), the membrane (K_m) and the gaseous permeate (K_p) as described in Eq. (1).

$$\frac{1}{K_o}=\frac{1}{K_f}+\frac{1}{K_m}+\frac{1}{K_p} \quad (1)$$

Where, K_o, K_f, K_m and K_p = the overall, the liquid feed water, the membrane, and the gaseous permeate mass transfer coefficient (in $s \cdot m^{-1}$), respectively.

K_p is negligible for vacuum stripping applications due to the low absolute pressure of the gaseous permeate, according to the studies of Bandini et al. [18], Lawson, et al. [19] and Jyoti et al. [12].

K_f can be determined as a function of the hydraulic conditions and the diffusion characteristics of the dissolved gases in the feed water [15, 20], but this is only applicable for uniform hydraulic conditions of the feed water. At the interface of the feed water and the membrane, the hydraulic conditions are different from those in the bulk phase, due to polarisation phenomena. For stripping of gases from water in vacuum configurations, three polarisation phenomena are relevant:

1. Temperature polarisation;

Table 1
Key characteristics of the membranes used for the NH_3 stripping experiments.

	Unit	Porous gas-permeable (PTFE) membrane	Hydrophilic (Hybrid Silica) PV membrane	Hydrophobic (PDMS) PV membrane
Channel height	mm	2.3	–	–
Channel width	mm	39	–	–
Internal diameter	mm	–	7	7
Membrane thickness	mm	0.2	1.5	1.5
Membrane length	mm	87	250	250
Effective membrane area	cm^2	34	55	55
Pore size[e]	nm	100	0.5 [17]	–
Selective membrane layer	–	PTFE[a]	Hybrid Silica – AR[c]	PDMS[d]
Membrane material	–	PTFE – PP[b]	α-Al_2O_3	α-Al_2O_3
Maximum temperature[e]	°C	82	150	70

[a] PTFE = polytetrafluoroethylene.
[b] PP = polypropylene.
[c] Hybrid Silica – AR = organic (methyl and ethanol) groups and silica [13].
[d] PDMS = polydimethylsiloxane.
[e] According to the supplier.

2. Ion accumulation concentration polarisation;
3. Gas depletion concentration polarisation;

Firstly, temperature polarisation, which is the decrease in temperature of the feed water at the membrane interface as a result of heat transport due to the evaporation of H_2O [19,21]. Secondly, accumulation concentration polarisation, describing the increase in concentration of non-volatile solutes such as ions at the membrane interface as a result of the evaporation of H_2O [19,21]. Thirdly, gas depletion concentration polarisation, which is the decrease in concentration of volatile solutes such as dissolved gases at the membrane interface, caused by a higher transfer rate of the respective gas through the membrane than the transfer rate from bulk-phase of the feed liquid to the membrane interface [18,22].

Finally, K_m depends on the type of membrane. For porous gas-permeable membranes, the main mass transfer mechanism is Knudsen diffusion because the ratio of the kinetic diameter of the gas molecule and pore size is smaller than 0.05 [4,19,23], whereas PV membranes are dense membranes for which the main mass transfer mechanisms rely on sorption/dissolution and diffusion [12]. In general, for both types of membranes, K_m is a function of the specific membrane characteristics, such as thickness, and the temperature of the membranes [12,19]. However, due to temperature polarisation, the actual temperature of the membrane is different from the temperature of the bulk phase of the liquid feed.

The mentioned three polarisation phenomena occur simultaneously during vacuum stripping of gases such as NH_3 from water and do not only affect the mass transfer coefficients K_f and K_m. The polarisation phenomena also affect the driving force of NH_3 and H_2O transfer, because the local accumulation of ions, the local depletion of dissolved NH_3 and the lower temperature at the membrane interface compared to the bulk feed water temperature affect the vapour pressures of NH_3 and H_2O at the liquid side of the membrane. To our best knowledge, understanding the mass transfer in vacuum membrane stripping processes, including all three polarisation phenomena and their interdependency is lacking in current literature. Therefore, in this study, we did not investigate the respective contribution of K_f and K_m separately, but only K_o.

To calculate the K_o of NH_3 ($K_{o,NH3}$), various studies used the logarithmic decrease in NH_3 concentration over time, in combination with the initial feed volume [4,6]. However, this method of determining the K_o only applies to the transfer of the solute (NH_3) and not to the solvent (H_2O). Moreover, this method assumes a fixed feed volume, whereas the feed water volumes decrease due to the evaporation of H_2O during the stripping process. Therefore, we determined the K_o for NH_3 and H_2O using the measured fluxes and the calculated vapour pressure difference, in line with the study of [12]. The NH_3 (Eq. (2)) and H_2O (Eq. (3)) fluxes were determined using the mass changes in the feed water over time. The vapour pressures of NH_3 and H_2O in the liquid feed were obtained by simulations using chemical equilibrium simulation software named PHREEQC, whereas the vapour pressures of NH_3 (Eq. (4)) and H_2O (Eq. (5)) in the gaseous permeate were calculated using the ratio of the fluxes and the absolute pressure of the permeate. More details on the determination of the fluxes can be found in our previous study [16]. Based on the NH_3 and H_2O fluxes and vapour pressures, the $K_{o,NH3}$ and $K_{o,H2O}$ were determined using Eq. (6) and Eq. (7), respectively. Finally, $S_{NH3/H2O}$ was determined using Eq. (6), as the ratio of $K_{o,NH3}$ and $K_{o,H2O}$, in line with Camus et al. [10] and Baker et al. [9].

$$J_{NH_3} = \frac{-(m_{NH_3,i+1} - m_{NH_3,i})}{A_m \cdot (t_{i+1} - t_i)} \quad (2)$$

$$J_{H_2O} = \frac{-(m_{H_2O,i+1} - m_{H_2O,i})}{A_m \cdot (t_{i+1} - t_i)} \quad (3)$$

Where, J_{NH3} and J_{H2O} = NH_3 and H_2O flux (in $kg \cdot m^{-2} \cdot s^{-1}$), $m_{NH3,i}$ and $m_{H2O,i}$ = NH_3 and H_2O mass at time instant 'i', respectively (in kg), A_m = membrane area (in m^2) and t_i = time instant 'i' (in s).

$$p_{p,NH_3} = \frac{J_{NH_3}}{J_{NH_3} + J_{H_2O}} \cdot p_p \quad (4)$$

$$p_{p,H_2O} = \frac{J_{H_2O}}{J_{NH_3} + J_{H_2O}} \cdot p_p \quad (5)$$

Where, $p_{p,NH3}$ and $p_{p,H2O}$ = vapour pressure of NH_3 and H_2O in the gaseous permeate, respectively (in Pa = $kg \cdot m^{-2} \cdot s^{-1}$) and p_p = permeate pressure (in Pa = $kg \cdot m^{-2} \cdot s^{-1}$, p_p = 1,500 Pa).

$$K_{o,NH_3} = \frac{J_{NH_3}}{p_{f,NH_3} - p_{p,NH_3}} \quad (6)$$

$$K_{o,H_2O} = \frac{J_{H_2O}}{p_{f,H_2O} - p_{p,H_2O}} \quad (7)$$

Where $K_{o,NH3}$ and $K_{o,H2O}$ = mass transfer coefficient of NH_3 and H_2O, respectively (in $s \cdot m^{-1}$) and $p_{f,NH3}$ and $p_{f,H2O}$ = vapour pressure of NH_3 and H_2O in the liquid feed water (in Pa = $kg \cdot m^{-2} \cdot s^{-1}$).

$$S_{NH_3/H_2O} = \frac{K_{NH_3}}{K_{H_2O}} \quad (8)$$

Where $S_{NH3/H2O}$ = selectivity of NH_3 over H_2O transfer (no unit).

2.3. Experimental conditions

For all conducted experiments in this study, the vacuum pressure at the permeate side was fixed at 1,500 Pa by a vacuum pump, while unsteady hydraulic flow conditions were maintained unless stated otherwise. Moreover, the temperature of the feed water was 35 °C, unless stated differently, because according to our previous study, stripping NH_3 at 35 °C resulted in the most concentrated NH_3 in the vapour permeate [16]. Initially, we assessed the transfer of H_2O through the various membranes at three different feed water temperatures: 25, 35 and 45 °C. Subsequently, unless stated differently, feed waters with a feed water concentration of 1 $g \cdot L^{-1}$ of NH_3 as NH_4OH were used to assess the $S_{NH3/H2O}$ for the various membranes, similar to Yang et al. [8] and Yang et al. [13].

2.3.1. Hydraulic conditions

We assessed the effect of the hydraulic conditions on the $S_{NH3/H2O}$, by using various Reynolds numbers, corresponding to steady (poorly mixed, or laminar) or unsteady (well-mixed, or transition/turbulent) hydraulic conditions. Unsteady flow conditions refer to the hydraulic flow conditions with good mixing properties. The unsteady flow conditions cover the range between laminar and turbulent hydraulic conditions. The Reynolds number is a function of the feed water properties, the cross-flow velocity and the hydraulic diameter of the flow channel (Eq. (9)). According to the study of Oliveira et al. [15], the hydraulic flow conditions are unsteady at a Reynolds number of 2,300 in tubular channels, whereas according to Mojab et al. [24] unsteady hydraulic conditions in spacer-filled channels correspond to a Reynolds number of 500. By taking the feed water properties into account, the Reynolds numbers were set by controlling the cross-flow velocity through the flow channels using the peristaltic pump.

$$Re = \frac{\rho_f \cdot u \cdot d_h}{\mu_f} \quad (9)$$

Where ρ_f = feed water density (in $kg \cdot m^{-3}$), u = average cross-flow velocity (in $m \cdot s^{-1}$), d_h = hydraulic diameter (in m), μ_w = dynamic viscosity of feed water (in $kg \cdot m^{-1} \cdot s^{-1}$).

The hydraulic diameter relates the surface tension and the shear stress of a liquid flowing through a channel. For circular open channels (for the tubular PV membranes), the hydraulic diameter is equal to the

diameter of the respective channel. For spacer-filled channels (for the flat-sheet PTFE membrane), the determination of the hydraulic diameter is more elaborate, as the liquid is in contact with both the spacer and the perimeter of the flow channel. To this end, Schock, et al. [25] proposed a general expression for the hydraulic diameter in spacer-filled channels (Eq. (8)), as a function of the void volume and the wetted surface area of the flow channel.

$$d_h = \frac{4 \cdot V_v}{A_w} \quad 10$$

Where, V_v = void volume (in m^3) and A_w = wetted surface area (in m^2).

The determination of the void volume and the wetted surface area of the flow channels as a function of the specific channel geometries are described in detail in the Supporting Information. The hydraulic diameters were 2.3 and 7.0 mm for the PTFE and PV membranes, respectively. For the PTFE membrane, the range of the cross-flow velocity was 8–20 cm•s^{-1} and 14–36 cm•s^{-1} for the PV membranes. The cross-flow velocities for the PTFE membrane to achieve unsteady hydraulic conditions are lower compared to the PV membranes, because the PTFE membrane is in contact with a spacer (to enhance mixing), while the PV membranes are open tubular channels.

2.3.2. Ammonia feed water concentration and ionic strength of the feed water

To the best of our knowledge, current literature mainly reports on the transfer of NH_3 from feed water through membranes, in which the NH_3 is only present as NH_4OH. Only the study of He et al. [6] and our previous study [16] did not use NH_4OH solutions as feed water, but used pre-treated biogas slurry and NH_4HCO_3 solutions at a pH of 10, respectively. Whereas 1 g•L^{-1} is a representative concentration of NH_3 in residual waters, 10 g•L^{-1} represents the concentration of NH_3 in pre-concentrated streams [1]. Obtaining NH_3 concentrations up to 10 g•L^{-1} can be achieved by using electrodialysis to concentrate NH_4^+ from 1.5 to 10 g•L^{-1} [26], followed by the addition of chemicals to increase the solution pH, or by using bipolar membrane electrodialysis to directly obtain concentrated NH_3 without chemical addition [27]. Because various nitrogen-rich residual waters, typically contain NH_4^+ in combination with HCO_3^- as the main anion, the addition of NaOH to obtain concentrated NH_3 from feed water with high NH_4^+ concentrations results in a high ionic strength, as a result of the presence of Na^+, HCO_3^- and CO_3^{2-}. The presence of ions affects the vapour pressure of NH_3 in two ways. On the one hand, when the ionic strength increases, the equilibrium between NH_4^+ and NH_3 shifts towards NH_4^+, according to chemical equilibrium simulations performed with PHREEQC software. On the other hand, the solubility of gases decreases when the ionic strength increases, which is called the salting-out effect, increasing the vapour pressure. According to Fig. 2, the vapour pressure of NH_3 increases linearly when the ionic strength of the feed water increases, indicating that the salting-out effect is stronger than the effect of the ionic strength on the equilibrium between NH_3 and NH_4^+. Furthermore, an increase in ionic strength results in a linear decrease in H_2O vapour pressure according to Raoult's Law. Hence, by increasing the ionic strength of the feed water, the NH_3 vapour pressure increases, while the H_2O vapour pressure decreases. The effect of the ionic strength on the vapour pressure of NH_3 and H_2O is similar for feed waters with NH_3 concentrations of 1 and 10 g•L^{-1}. However, in addition to the effect of the ionic strength on the vapour pressures, the ionic strength also affects the resistance to mass transfer of NH_3 and H_2O. Due to the evaporation of H_2O, ions accumulate at the membrane interface (ion accumulation concentration polarisation), which can hinder the transfer of NH_3 and H_2O, particularly under steady hydraulic conditions.

We assessed the effect of ionic strength on $S_{NH3/H2O}$, because the presence of ions affects both the vapour pressure of dissolved gases (salting-out effect) and the mass transfer coefficient (ion accumulation concentration polarisation). To assess the effect of the NH_3 feed concentration and ionic strength on $S_{NH3/H2O}$, we prepared various feed waters containing dissolved NH_3 with initial concentrations of 1 and 10 g•L^{-1} as NH_4OH and NH_4HCO_3 (at a pH of 10 by addition of NaOH). According chemical equilibrium simulations, the ionic strength of feed water consisting of NH_4OH is negligible, whereas feed waters consisting of NH_4HCO_3 at a pH of 10 have an ionic strength of 0.1 and 0.8 mol•L^{-1} at NH_3 feed water concentration of 1 and 10 g•L^{-1}, respectively. For these calculations, the contribution of both NH_4HCO_3 and NaOH to the ionic strength were taken into account.

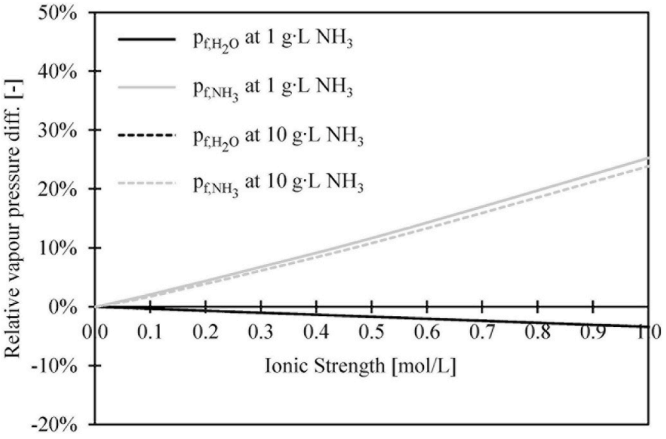

Fig. 2. The calculated vapour pressures of NH_3 and H_2O in water with an NH_3 feed water concentration of 1 and 10 g•L^{-1}, as a function of the ionic strength of the feed water. The vapour pressures were calculated using PHREEQC simulation software, using the phreeqc.dat database.

3. Results and discussion

3.1. Water transfer through the various membranes as a function of the feed temperature

Initially, the transfer rate of H_2O as the H_2O flux and the $K_{o,H2O}$ through the membranes was assessed at various temperatures, using water as a feed without dissolved gaseous and ions, at unsteady hydraulic conditions. Fig. 3A presents the H_2O fluxes as a function of the feed water temperature for the PTFE, Hybrid Silica PV and PDMS PV membrane. The reported values represent averages of at least triplicate experimental runs. At a feed water temperature of 25 °C, the H_2O flux for the PTFE membrane was 12.0 kg•m^{-2}•h^{-1}, compared to 2.3 and 0.4 kg•m^{-2}•h^{-1} for the Hybrid Silica PV and PDMS PV membrane, respectively. By increasing the feed water temperature to 45 °C, the H_2O fluxes increased to 24.5, 6.3 and 0.7 kg•m^{-2}•h^{-1} for the PTFE, Hybrid Silica PV and PDMS PV membranes, respectively, because the vapour pressure of H_2O and thus the driving force increased as a function of temperature. The H_2O flux for the PTFE membrane was at least four times higher than the H_2O flux for the Hybrid Silica PV membrane, which in its turn was at least five times higher than the H_2O flux of the PDMS PV membrane.

Because the same feed water temperature range and same vacuum pressure were applied for the experiments, the higher H_2O fluxes of the PTFE membrane compared to the PV membranes are explained by the higher $K_{o,H2O}$ of the PTFE membrane (ranging between $1 \cdot 10^{-6}$ and $2 \cdot 10^{-6}$ s•m^{-1}) compared to the $K_{o,H2O}$ of the Hybrid Silica PV (ranging between $2 \cdot 10^{-7}$ and $4 \cdot 10^{-7}$ s•m^{-1}) and the PDMS PV membrane (ranging between $7 \cdot 10^{-8}$ and $2 \cdot 10^{-7}$ s•m^{-1}), as presented in Fig. 3B. The difference in $K_{o,H2O}$ between the PTFE membrane and the PV membranes can be assigned to the differences in selective layers of the membranes. The PTFE membrane had pores of 0.1 μm, whereas the Hybrid Silica PV and PDMS PV membranes were dense membranes, resulting in lower transfer rates of H_2O than compared to the porous PTFE membrane. The difference in $K_{o,H2O}$ between the Hybrid Silica PV

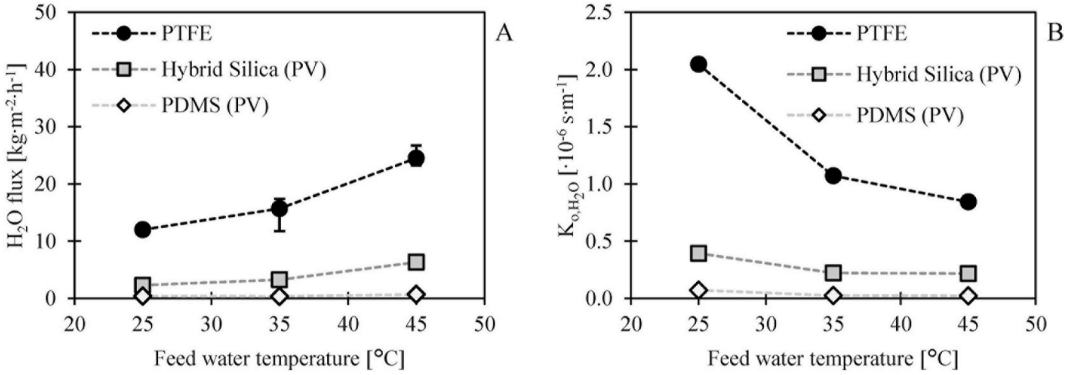

Fig. 3. (A) The H_2O fluxes and (B) the $K_{o,H2O}$ of the gas permeable PTFE membrane and the hydrophilic Hybrid Silica PV and hydrophobic PV membrane as a function of the feed water temperature. The reported values and error bars represent average and the minimum and maximum measurements of at least three replicate experiments.

and the PDMS PV membrane can be explained by the functional groups present in the selective layers of the respective membranes. The selective layer of the Hybrid Silica PV membrane was hydrophilic and contained polar organosilica groups, allowing for the permeation of polar H_2O molecules. On the contrary, the selective layer of the PDMS PV membrane was hydrophobic, which hindered the dissolution of H_2O in the membrane and the subsequent diffusion of H_2O through the membrane.

According to Fig. 3B, the $K_{o,H2O}$ of all three membranes decreased when the feed water temperature increased. The decrease of $K_{o,H2O}$ as a function of the increasing feed water temperature can be assigned to a stronger effect of temperature polarisation [21], as no ions or dissolved gases were present in the feed water. For the PTFE membrane, the decrease in $K_{o,H2O}$ as a function of the feed water temperature can be assigned to the decrease in K_m, which decreases as a function of the temperature according to Knudsen diffusion. In addition, for the PV membranes, the mass transfer through the membranes can be described by sorption-diffusion models. When the temperature increases, diffusion increases, while sorption decreases. Therefore, the decrease in $K_{o,H2O}$ of the PV membranes as a function of the increasing feed water temperature may, besides temperature polarisation, also be caused by the effect of the feed water temperature on the sorption and diffusion mechanisms taking place during the transfer of H_2O. However, because the temperature at the interface of the liquid feed water and the membranes was not determined, it remains unclear which component of the series resistance model for mass transfer (Eq. (1)) caused the decrease of the $K_{o,H2O}$ as a function of the increasing feed water temperature.

3.2. Selectivity of ammonia over water transfer of various membranes

Fig. 4A presents the fluxes of both NH_3 and H_2O for the various membranes. The H_2O and NH_3 fluxes of the PTFE membrane were 11 and 0.11 kg•m^{-2}•h^{-1}, respectively. For the Hybrid Silica PV membrane, the H_2O flux was 4 kg•m^{-2}•h^{-1} and the NH_3 flux was 0.02 kg•m^{-2}•h^{-1}. Furthermore, the H_2O flux for the PDMS PV membrane was 1 kg•m^{-2}•h^{-1}, but the NH_3 flux was negligible. Moreover, the selective layer of the PDMS PV membrane deteriorated rapidly during the experiments (see Fig. 5), indicating that treating alkaline feed waters with an NH_3 concentration of 1 g•L^{-1} was not possible for periods exceeding 3 h. Therefore, we did not further assess the applicability of the PDMS PV membrane.

The $K_{o,H2O}$ of the Hybrid Silica PV ($3•10^{-8}$ s•m^{-1}) and PDMS PV ($7•10^{-8}$ s•m^{-1}) membranes were again (also in 3.1) lower compared to the PTFE membrane $K_{o,H2O}$ ($8•10^{-7}$ s•m^{-1}), caused by the lower resistance of H_2O transfer through the PTFE membrane. The lower resistance of H_2O transfer for the PTFE membrane compared to the Hybrid Silica PV membrane, which is expressed as higher H_2O flux and higher $K_{o,H2O}$,

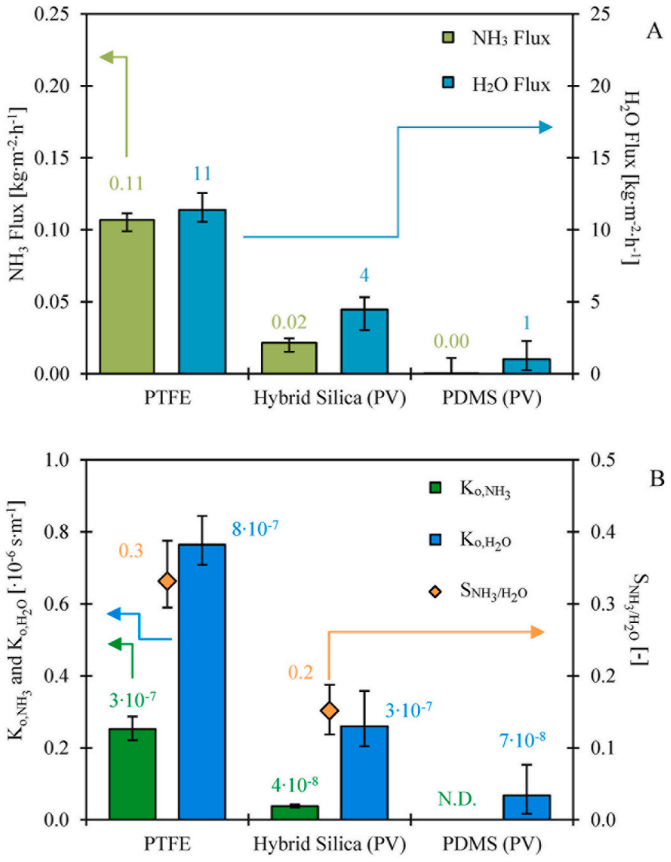

Fig. 4. (A) The NH_3 and H_2O fluxes and (B) the $K_{o,NH3}$, $K_{o,H2O}$ and $S_{NH3/H2O}$ of the various membranes for stripping NH_3 from feed waters with an NH_3 feed concentration of 1 g•L^{-1} (as NH_4OH) at a feed water temperature of 35 °C at unsteady hydraulic conditions. The reported values and error bars represent average and the minimum and maximum measurements of at least three replicate experiments. N.D. = not determined (too low flux).

can mainly be assigned to the membrane characteristics. According to Table 1, the pore size of the PTFE membrane was orders of magnitude higher compared to the PV membranes, while also the membrane thickness of the PTFE membrane was lower compared to the PV membranes. Hence, both the higher pore size and the lower membrane thickness contributed to the higher H_2O transfer rates through the PTFE membrane compared to the PV membranes. Furthermore, the $K_{o,NH3}$ of the PTFE membrane ($3•10^{-7}$ s•m^{-1}) was more than seven times higher than the Hybrid Silica PV ($4•10^{-7}$ s•m^{-1}). The differences in NH_3 flux

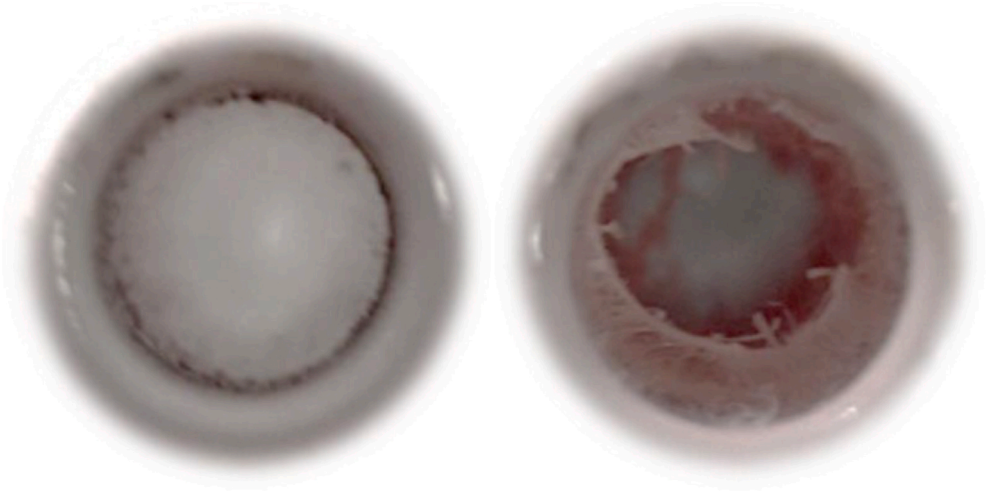

Fig. 5. A new PDMS PV membrane (left) and a deteriorated PDMS PV membrane (right) after exposure to feed water of 35 °C with an NH_3 concentration of 1 g L^{-1} for less than 6 h.

and $K_{o,NH3}$ between the PTFE membrane and Hybrid Silica PV membrane can again be assigned to the pore size and the thickness of the respective membranes. Due to the negligible NH_3 flux, the $K_{o,NH3}$ of the PDMS PV membrane was not determined.

The PTFE membrane showed a preference to permeate H_2O over NH_3 indicated by the $S_{NH3/H2O}$ of 0.3. The $S_{NH3/H2O}$ of the PTFE membrane was higher than the $S_{NH3/H2O}$ of the Hybrid Silica PV membrane (0.2). Hence, the Hybrid Silica PV did not show an increased preference to permeate NH_3 compared to H_2O, in contrast to the findings of Yang et al. [8], but in line with the findings of Yang et al. [13]. The adsorption of NH_3 on the silica groups of the PV membranes, leading to blocking of the H_2O transfer, as described by Yang et al. [8], was not present or not strong enough to promote selective NH_3 permeation. This blocking mechanism was responsible for the selective transfer of NH_3 over H_2 in studies conducted by Camus et al. [10] and Kanezashi et al. [11]. However, in contrast to the non-polar H_2, NH_3 (dipole moment of 1.47 D) and H_2O (dipole moment of 1.85 D) are both polar molecules [28] and both bind with the polar silica groups at the selective layer of the Hybrid Silica PV membrane. In fact, H_2O is more polar than NH_3 and probably bonded stronger with the selective layer of the Hybrid Silica PV membrane, contributing to the lower $S_{NH3/H2O}$. Furthermore, H_2O was more abundantly present in the bulk phase of the feed water than NH_3 (>99 wt%), as the feed water NH_3 concentration was 1 g L^{-1}, corresponding to 0.1 wt%. Therefore, also gas depletion concentration polarisation affected the transfer of NH_3, possibly explaining the preference of H_2O over NH_3 transfer.

3.3. Selectivity of ammonia over water under various hydraulic conditions

3.3.1. Identification of hydraulic condition ranges

According to the studies of Oliveira et al. [15] and Mojab et al. [24], unsteady flow regions for tubular and spacer-filled channels start at a Reynolds number of 2,300 and 500, respectively. Fig. 6A and B presents the H_2O flux as a function of the Reynolds number for the PTFE and the Hybrid Silica PV membrane, respectively, when using demineralised water as feed water. For the PTFE membrane, the H_2O flux was 11 $kg \cdot m^{-2} \cdot h^{-1}$ up to a Reynolds number of 300. The H_2O flux increased to 15 $kg \cdot m^{-2} \cdot h^{-1}$ when the Reynolds number increased to 400 and remained stable when the Reynolds number further increased to 500 and 600. For the Hybrid Silica PV membrane, the H_2O flux increased from 3 to 4 $kg \cdot m^{-2} \cdot h^{-1}$ when the Reynolds number increased from 1,000 to 2,400 and remained 4 $kg \cdot m^{-2} \cdot h^{-1}$ when the Reynolds number further increased to 3,000, 4,000 and 5,000. Hence, the indicated Reynolds numbers for steady and unsteady hydraulic conditions were in line with the changes in H_2O flux for both spacer-filled rectangular and open tubular channels [15,24].

Because during the H_2O permeation experiments at various Reynolds numbers the driving force for H_2O transfer was equal, as the same feed water temperature and vacuum pressure were used, the increase in H_2O

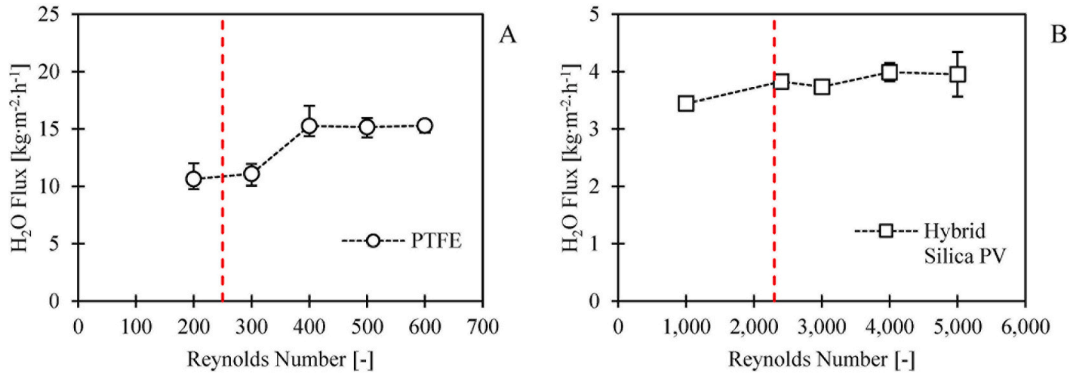

Fig. 6. (A) The H_2O flux of the PTFE membrane and (B) the Hybrid Silica PV membrane (PV) at a feed water temperature of 35 °C as a function of the Reynolds numbers. The dotted vertical lines represent the Reynolds numbers at which theoretically the hydraulic conditions become unsteady: 250 for spacer-filled rectangular flow channels and 2,300 for tubular flow channels. The reported values and error bars represent average and the minimum and maximum measurements of at least three replicate experiments.

flux due to the shift from steady to unsteady hydraulic conditions was caused by an increase in $K_{o,H2O}$. By shifting from steady to unsteady hydraulic conditions, the effect of temperature polarisation was less apparent, resulting in a higher feed vapour pressure at the membrane interface and thus actual driving force for H_2O transfer. Moreover, as the membrane temperature was probably higher at higher Reynolds numbers due to the weaker effect of temperature polarisation, the K_m for the PTFE decreased, according to mass transfer described Knudsen diffusion. Apparently, the increase in actual H_2O driving force had a greater impact than the decrease in K_m on the H_2O flux. For the Hybrid Silica PV membrane, the increase in Reynolds number probably resulted into an increased actual H_2O driving force, as well as an increased K_m, due to the reduced effect of temperature polarisation, ultimately leading to an increase in H_2O flux.

3.3.2. Selectivity of ammonia over water under steady and unsteady hydraulic conditions

Subsequently, NH_3 transfer was assessed under both steady and unsteady hydraulic conditions for the PTFE and the Hybrid Silica PV membranes. Based on results of H_2O transfer as a function of the Reynolds number experiments (see Section 3.3.1.), we used Reynolds numbers of 200 and 500 for the PTFE membrane and 1,000 and 2,400 for the Hybrid Silica PV membrane as representative values of steady and unsteady hydraulic conditions, respectively. In line with the findings in Section 3.2., the transfer rates of NH_3 and H_2O, expressed as flux and K_o were consistently lower for the Hybrid Silica PV membrane, compared to the PTFE membrane, which can be explained by the membrane thickness and pore size of the respective membranes.

Fig. 7A shows that the NH_3 flux for the PTFE membrane increased from 0.08 to 0.11 $kg \cdot m^{-2} \cdot h^{-1}$ when the hydraulic conditions shifted from steady to unsteady, whereas for the Hybrid Silica PV the NH_3 flux increased from 0.01 to 0.02 $kg \cdot m^{-2} \cdot h^{-1}$. The H_2O fluxes for the PTFE and Hybrid Silica PV membrane remained stable at 11 and 3 $kg \cdot m^{-2} \cdot h^{-1}$, respectively, when the hydraulic conditions shifted from steady to unsteady. The rate of H_2O transfer during the experiments with demineralised water in Section 3.1 and Section 3.3.1. was consistently higher compared to the experiments using feed waters containing NH_4OH, indicating that the transfer of NH_3 affected the transfer of H_2O. Furthermore, the shift from steady to unsteady hydraulic conditions had a greater impact on the $K_{o,NH3}$ than on the $K_{o,H2O}$. The $K_{o,NH3}$ increased from $1 \cdot 10^{-7}$ to $3 \cdot 10^{-7}$ $s \cdot m^{-1}$ and from $2 \cdot 10^{-8}$ to $3 \cdot 10^{-8}$ $s \cdot m^{-1}$ for the PTFE and the Hybrid Silica PV membrane, respectively, whereas the $K_{o,H2O}$ remained at $7 \cdot 10^{-7}$ - $8 \cdot 10^{-7}$ $s \cdot m^{-1}$ and $2 \cdot 10^{-7}$ $s \cdot m^{-1}$, respectively. The increase in NH_3 fluxes and $K_{o,NH3}$ by shifting from steady to unsteady hydraulic conditions can be explained by a decrease in the effect of gas depletion concentration polarisation.

The $S_{NH3/H2O}$ increased when the hydraulic conditions shifted from steady to unsteady conditions, in line with the findings of Ding et al. [3] and El-Bourawi et al. [4]. For the PTFE membrane, $S_{NH3/H2O}$ increased from 0.2 to 0.3, while $S_{NH3/H2O}$ for the Hybrid Silica PV membrane increased from 0.1 to 0.2, indicating that the PTFE membrane again had a higher selectivity for NH_3 over H_2O transfer than the Hybrid Silica PV membrane, in line with the findings described in Section 3.2. The observed increase in $S_{NH3/H2O}$ for the PTFE membrane contradicted to the observations of He et al. [6], who found that $K_{o,H2O}$ increased more than $K_{o,NH3}$ for higher cross-flow velocities. However, it was unclear whether these experiments were conducted in either steady or unsteady hydraulic conditions as the hydraulic diameter and geometry of the feed channel were not reported. Hence, our observations show that stripping NH_3 at unsteady hydraulic conditions were preferred over operating at steady hydraulic conditions to maximise $S_{NH3/H2O}$, irrespective of the used type of membrane, also in line with the findings of Scheepers et al. [7].

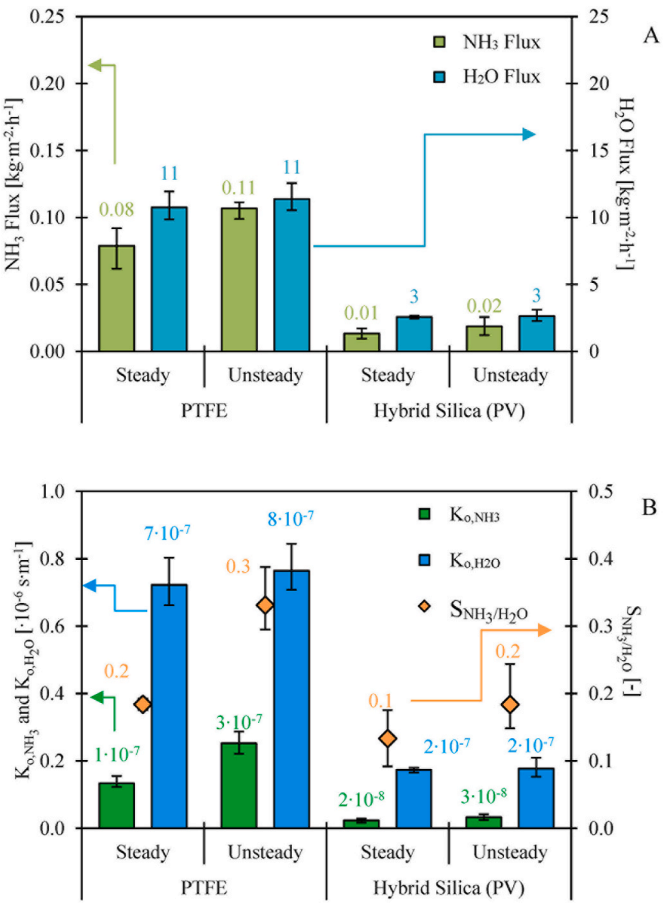

Fig. 7. (A) The NH_3 and H_2O fluxes and (B) the $K_{o,NH3}$, $K_{o,H2O}$ and $S_{NH3/H2O}$ of the PTFE and the hydrophilic Hybrid Silica PV membrane for stripping NH_3 for steady and unsteady hydraulic conditions, from feed waters with an NH_3 feed concentration of 1 $g \cdot L^{-1}$ (as NH_4OH) at a feed water temperature of 35 °C at both steady and unsteady hydraulic conditions. The reported values and error bars represent average and the minimum and maximum measurements of at least three replicate experiments.

3.4. Selectivity of ammonia over water of various membranes for various feed water compositions

3.4.1. Ammonia feed water concentration of 1 $g \cdot L^{-1}$ at various ionic strengths

Fig. 8A shows that the fluxes of NH_3 for the PTFE membrane were 0.11 and 0.14 $kg \cdot m^{-2} \cdot h^{-1}$ when feed waters had a negligible ionic strength (NH_4OH) and an ionic strength of 0.1 $mol \cdot L^{-1}$ (NH_4HCO_3 at a pH of 10), respectively. The H_2O flux of the PTFE membrane ranged between 11 and 12 $kg \cdot m^{-2} \cdot h^{-1}$ for the feed waters with negligible and 0.1 $mol \cdot L^{-1}$ ionic strengths, respectively, while the $K_{o,H2O}$ was $8 \cdot 10^{-7}$ $s \cdot m^{-1}$ (see Fig. 8B). Based on the ratio of the NH_3 and H_2O fluxes (0.01), the energy consumption can be derived, based on our previous study [5]. The energy consumption for stripping NH_3 at an NH_3 feed water concentration of 1 $g \cdot L^{-1}$ was approximately 100 MJ•kg-N^{-1}. According to Fig. 8B, the $K_{o,NH3}$ was $3 \cdot 10^{-7}$ $s \cdot m^{-1}$ for both feed waters, indicating that the effect of the difference in ionic strength of 0.1 $mol \cdot L^{-1}$ was negligible on the NH_3 transfer. The $S_{NH3/H2O}$ for the PTFE membrane for these experiments ranged between 0.3 and 0.4, which indicates the transfer of H_2O was again preferential over NH_3 (similar as in Section 3.2 and 3.3), independent of the difference in ionic strength. In addition, in line with the findings in Section 3.2. and Section 3.3., the transfer rates of NH_3 and H_2O, expressed as flux and K_o were consistently lower for the Hybrid Silica PV membrane, compared to the PTFE membrane, which can be explained by the membrane thickness and pore size of the

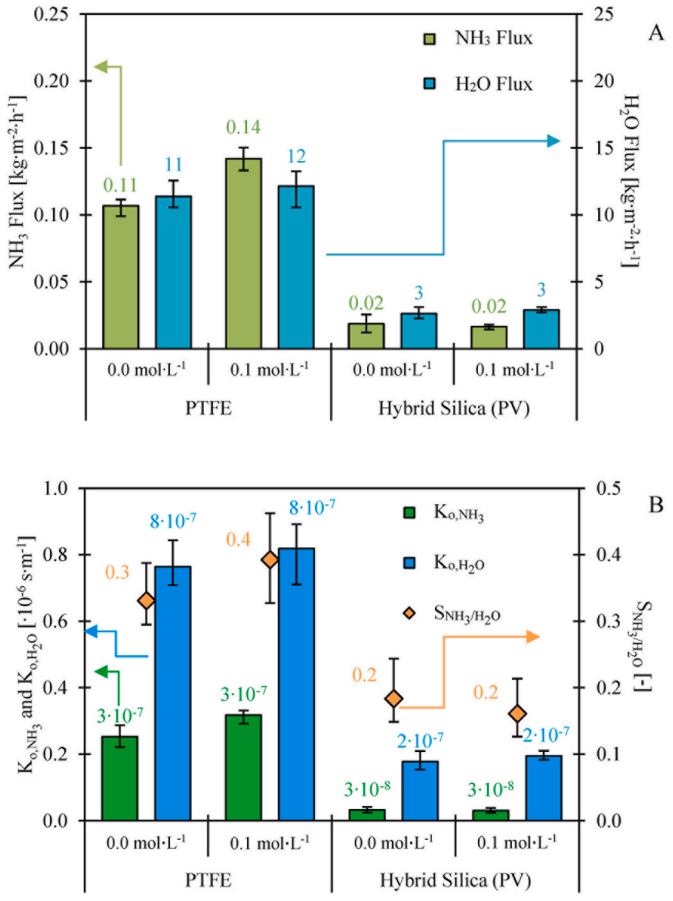

Fig. 8. (A) The NH_3 and H_2O fluxes and (B) the $K_{o,NH3}$, $K_{o,H2O}$ and $S_{NH3/H2O}$ of the PTFE and the Hybrid Silica PV membrane for stripping NH_3 from feed waters with an NH_3 feed concentration of 1 g•L^{-1} having a negligible (as NH_4OH) and 0.8 mol•L^{-1} (as NH_4HCO_3 at a pH of 10) ionic strength at a feed water temperature of 35 °C at unsteady hydraulic conditions. The reported values and error bars represent average and the minimum and maximum measurements of at least three replicate experiments.

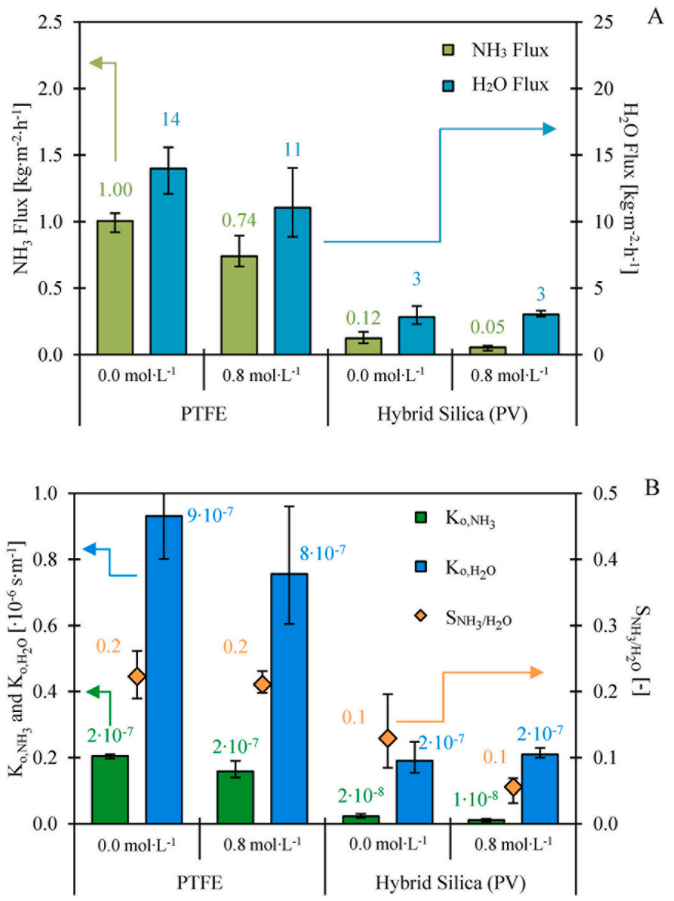

Fig. 9. (A) The NH_3 and H_2O fluxes and (B) the $K_{o,NH3}$, $K_{o,H2O}$ and $S_{NH3/H2O}$ of the PTFE and the Hybrid Silica PV membrane for stripping NH_3 from feed waters with an NH_3 feed concentration of 10 g•L^{-1} having a negligible (as NH_4OH) and 0.8 mol•L^{-1} (as NH_4HCO_3 at a pH of 10) ionic strength at a feed water temperature of 35 °C at unsteady hydraulic conditions. The reported values and error bars represent average and the minimum and maximum measurements of at least three replicate experiments.

respective membranes.

For the Hybrid Silica PV membrane, the NH_3 and H_2O fluxes were 0.02 and 3 kg•m^{-2}•h^{-1}, respectively, when using feed water with a negligible and 0.1 mol•L^{-1} ionic strength at an NH_3 feed concentration of 1 g•L^{-1}. The $K_{o,H2O}$ of the Hybrid Silica PV membrane for the feed water with different ionic strengths was $2•10^{-7}$ s•m^{-1} and the $K_{o,NH3}$ was $3•10^{-8}$ s•m^{-1}. The $S_{NH3/H2O}$ of the Hybrid Silica PV membrane for both feed waters was 0.2, suggesting that the increase in ionic strength of 0.1 mol•L^{-1} did not affect the selectivity of NH_3 over H_2O transfer, which is in agreement with the findings for the PTFE membrane.

3.4.2. Ammonia feed water concentration of 10 g•L^{-1} at various ionic strengths

At last, the $S_{NH3/H2O}$ was assessed for the PTFE and Hybrid Silica PV membrane using feed waters with an NH_3 feed concentration of 10 g•L^{-1} with a negligible ionic strength (NH_4OH) and an ionic strength of 0.8 mol•L^{-1} (NH_4HCO_3 at a pH of 10). The NH_3 fluxes for the PTFE membrane were 1.00 and 0.74 kg•m^{-2}•h^{-1} for the feed waters with a negligible and 0.8 mol•L^{-1} ionic strength, respectively, whereas the H_2O fluxes were 14 and 11 kg•m^{-2}•h^{-1}, respectively (see Fig. 9A). Hence, the fluxes of both NH_3 and H_2O decreased when the ionic strength of the feed water increased from 0.0 to 0.8 mol•L^{-1}. With a ratio of the NH_3 flux and the total flux of 0.06, the electrical energy consumption for stripping NH_3 at an NH_3 feed water concentration of 10 g•L^{-1} was approximately 10 MJ•kg-N^{-1}, based on [5]. For the Hybrid Silica PV membrane, the NH_3 flux was 0.12 and 0.05 kg•m^{-2}•h^{-1} for feed waters with a negligible and 0.8 mol•L^{-1} ionic strength, respectively, while the H_2O flux was stable for both feed waters at 3 kg•m^{-2}•h^{-1}. In line with the findings on the PTFE membrane, the NH_3 flux also decreased for the Hybrid Silica PV membrane when the ionic strength increased from 0.0 to 0.8 mol•L^{-1} for feed water with an NH_3 feed concentration of 10 g•L^{-1}.

According to Fig. 9B, the $K_{o,NH3}$ ($2•10^{-7}$ s•m^{-1}) for the PTFE membrane did not change when the ionic strength increased from 0.0 to 0.8 mol•L^{-1}, suggesting that the additional presence of ions did not affect the NH_3 transfer. In addition, the increase in ionic strength also did not affect the transfer of H_2O for the PTFE membrane, as the $K_{o,H2O}$ ($8•10^{-7}$ - $9•10^{-7}$ s•m^{-1}) was similar for a negligible and 0.8 mol•L^{-1} ionic strength. Eventually, the $S_{NH3/H2O}$ was 0.2 for feed water with an NH_3 feed water concentration of 10 g•L^{-1} with both a negligible and 0.8 mol•L^{-1} ionic strength, indicating that the selectivity of NH_3 transfer was not affected by the increase in ionic strength for the PTFE membrane. For the Hybrid Silica PV membrane, the $K_{o,NH3}$ decreased from $2•10^{-8}$ to $1•10^{-8}$ s•m^{-1} when the ionic strength increased from 0.0 to 0.8 mol•L^{-1}, while $K_{o,H2O}$ for the Hybrid Silica PV membrane was stable at $2•10^{-7}$ s•m^{-1}. Hence, the increase in ionic strength of 0.8 mol•L^{-1} affected only the transfer of NH_3, which can be assigned to the increased effect of gas depletion concentration polarisation. Eventually, the $S_{NH3/H2O}$ for the Hybrid Silica was 0.1 for an NH_3 feed water concentration of 10 g•L^{-1} with both a negligible and 0.8 g•L^{-1} ionic strength.

By increasing the NH_3 feed concentration from 1 to 10 g•L^{-1}, the NH_3 flux increased for the PTFE membrane from 0.08 to 0.11 to 0.74–1.00 kg•m^{-2}•h^{-1}, in line with the study of Scheepers et al. [7] However, the $K_{o,NH3}$ of the PTFE membrane decreased when increasing the NH_3 feed water concentration, while the $K_{o,H2O}$ remained equal, resulting in a decrease in $S_{NH3/H2O}$ from 0.3 to 0.4 to 0.2. In line with the findings for the PTFE membrane, also the $S_{NH3/H2O}$ for the Hybrid Silica decreased when the NH_3 feed water concentration increased from 1 to 10 g•L^{-1}, from 0.2 to 0.1, respectively. Hence, the increases in NH_3 flux for both the PTFE and Hybrid Silica PV membrane when the NH_3 feed water concentration increased from 1 to 10 g•L^{-1} was caused by the higher driving force as a result of the higher NH_3 vapour pressure in the feed water. Moreover, the selectivity of NH_3 transfer over H_2O decreased further for both membranes when the NH_3 feed water concentration increased. Apparently, even at a ten-fold higher NH_3 feed concentration, the relative presence of NH_3 was low (approximately 1 wt%) compared to H_2O, explaining partially the preferential transfer of H_2O over NH_3 for both membranes, under all various feed water compositions.

3.5. Future outlook

The selected silica-based PV membranes did not allow for selective transfer of NH_3 over H_2O during the vacuum stripping of NH_3 from various feed waters. In fact, the used PV membranes even did not have a higher $S_{NH3/H2O}$ than the used porous PTFE membrane. A major restriction is the similarity between NH_3 and H_2O in terms of molecular weight (17 and 18 g•mol^{-1}, respectively), kinetic diameter (0.33 and 0.26 nm, respectively) and polarity (dipole moment of 1.47 and 1.85 D, respectively). Furthermore, since H_2O was abundantly present (approximately 99 wt% in this study) in the used feed waters, it was not feasible to achieve preferential NH_3 transfer with the used membranes and operational conditions. In contrast to previous literature, the hydrophilic PV membrane showed a preference for H_2O, while for the hydrophobic PV membrane the NH_3 transfer was negligible and the selective layer rapidly deteriorated when being exposed to NH_3 feed water. Hence, new membrane materials are needed to allow for selective permeation of NH_3 over H_2O, for example as a selective layer of dense membranes. The materials of the selective layer of the membrane should either avoid the dissolution of H_2O and allow for solution and diffusion of NH_3, or allow for solution and diffusion of NH_3 and strong binding of H_2O on the selective layer without blocking the transfer of NH_3. To develop new membrane materials that allow for more selective NH_3 over H_2O transfer, advantage of the difference in acidity coefficients (pK_a) between NH_3 and H_2O can be made. By allowing for less strong bonding of NH_3 than H_2O to the membrane material after sorption due to the differences in pK_a, potentially higher transfer rates of NH_3 compared to H_2O can be established. To support the development of new membrane materials for more selective NH_3 over H_2O transfer, we think more research on the surface affinity between NH_3 and H_2O and membrane materials is needed. Finally, in contrast to the PDMS PV membrane, the respective selective layer must be resistant to alkaline aqueous conditions.

4. Conclusions

Based on the experiments to assess the $S_{NH3/H2O}$ of various membranes while stripping NH_3 from water under different hydraulic conditions and for various feed water compositions, we can conclude the following:

- The transfer rate of H_2O (as H_2O flux and $K_{o,H2O}$) through the used dense hydrophilic Hybrid Silica PV membrane is lower than the transfer rate of H_2O of the used porous gas-permeable PTFE membrane;
- The transfer rate of H_2O through the used dense hydrophobic PDMS PV membrane is lower than the transfer rate of H_2O of the Hybrid Silica PV and the PTFE membrane;
- The transfer of NH_3 through the PMDS PV membrane is negligible and the membrane deteriorates rapidly when using feed waters containing NH_3;
- The used PTFE membrane and Hybrid Silica PV membranes show selectivity for transfer of H_2O over NH_3 for all tested hydraulic conditions and feed water compositions;
- The $S_{NH3/H2O}$ of the Hybrid Silica PV membrane (0.1–0.2) is consistently lower than the $S_{NH3/H2O}$ of the used PTFE membrane (0.2–0.4);
- Unsteady hydraulic conditions result in a higher $S_{NH3/H2O}$ compared to steady hydraulic conditions for both the PTFE and the Hybrid Silica PV membrane;
- An increase in ionic strength of the feed water from 0.0 to 0.8 mol•L^{-1} decreases the $S_{NH3/H2O}$ of both the PTFE and the Hybrid Silica PV membrane;
- An increase in NH_3 feed concentration from 1 to 10 g•L^{-1} leads to a decrease in $S_{NH3/H2O}$ for both the PTFE and the Hybrid Silica PV membrane;

CRediT authorship contribution statement

Niels van Linden: Investigation, Conceptualization, Methodology, Validation, Investigation, Writing – original draft, Visualization. **Yundan Wang:** Investigation, Conceptualization, Methodology, Investigation. **Ernst Sudhölter:** Conceptualization, Validation, Writing – review & editing. **Henri Spanjers:** Funding acquisition, Supervision, Writing – review & editing. **Jules B. van Lier:** Funding acquisition, Supervision, Writing – review & editing.

Declaration of competing interest

The authors declare no competing financial interest.

Acknowledgements

This study is part of the N2kWh – From Pollutant to Power research (14712), funded by the Netherlands Organisation for Scientific Research (NWO) (former Stichting voor Technische Wetenschappen (STW)); and Agentschap Innoveren & Ondernemen (VLAIO) (former Instituut voor Innovatie door Wetenschap en Technologie (IWT)). In addition, we thank E. Martens and L. Kattenberg for their contributions concerning the execution of the experiments.

Appendix A. Supplementary data

Supplementary data to this article can be found online at https://doi.org/10.1016/j.memsci.2021.120005.

References

[1] Z. Deng, N. van Linden, E. Guillen, H. Spanjers, J.B. van Lier, Recovery and applications of ammoniacal nitrogen from nitrogen-loaded residual streams: a review, J. Environ. Manag. 295 (2021) 113096.
[2] V. Vasilaki, T.M. Massara, P. Stanchev, F. Fatone, E. Katsou, A decade of nitrous oxide (N2O) monitoring in full-scale wastewater treatment processes: a critical review, Water Res. 161 (2019) 392–412.
[3] Z. Ding, L. Liu, Z. Li, R. Ma, Z. Yang, Experimental study of ammonia removal from water by membrane distillation (MD): the comparison of three configurations, J. Membr. Sci. 286 (2006) 93–103.
[4] M.S. El-Bourawi, M. Khayet, R. Ma, Z. Ding, Z. Li, X. Zhang, Application of vacuum membrane distillation for ammonia removal, J. Membr. Sci. 301 (2007) 200–209.
[5] N. van Linden, H. Spanjers, J.B. van Lier, Fuelling a solid oxide fuel cell with ammonia recovered from water by vacuum membrane stripping, Chem. Eng. J. 428 (2022) 131081.
[6] Q. He, T. Tu, S. Yan, X. Yang, M. Duke, Y. Zhang, S. Zhao, Relating water vapor transfer to ammonia recovery from biogas slurry by vacuum membrane distillation, Separ. Purif. Technol. 191 (2018) 182–191.

[7] D.M. Scheepers, A.J. Tahir, C. Brunner, E. Guillen-Burrieza, Vacuum membrane distillation multi-component numerical model for ammonia recovery from liquid streams, J. Membr. Sci. 614 (2020) 118399.
[8] X. Yang, T. Fraser, D. Myat, S. Smart, J. Zhang, J.C. Diniz da Costa, A. Liubinas, M. Duke, A pervaporation study of ammonia solutions using molecular sieve silica membranes, Membranes 4 (2014) 40–54.
[9] R.W. Baker, J.G. Wijmans, Y. Huang, Permeability, permeance and selectivity: a preferred way of reporting pervaporation performance data, J. Membr. Sci. 348 (2010) 346–352.
[10] O. Camus, S. Perera, B. Crittenden, Y.C. van Delft, D.F. Meyer, P.P.A.C. Pex, I. Kumakiri, S. Miachon, J.-A. Dalmon, S. Tennison, P. Chanaud, E. Groensmit, W. Nobel, Ceramic membranes for ammonia recovery, AIChE J. 52 (2006) 2055–2065.
[11] M. Kanezashi, A. Yamamoto, T. Yoshioka, T. Tsuru, Characteristics of ammonia permeation through porous silica membranes, AIChE J. 56 (2010) 1204–1212.
[12] G. Jyoti, A. Keshav, J. Anandkumar, Review on pervaporation: theory, membrane performance, and application to intensification of esterification reaction, J. Eng. (2015) 24, 2015.
[13] X. Yang, L. Ding, M. Wolf, F. Velterop, H.J.M. Bouwmeester, S. Smart, J.C. Diniz da Costa, A. Liubinas, J.-D. Li, J. Zhang, M. Duke, Pervaporation of ammonia solution with γ-alumina supported organosilica membranes, Separ. Purif. Technol. 168 (2016) 141–151.
[14] X. Yang, S. Sheridan, L. Ding, D.K. Wang, S. Smart, J.C. Diniz da Costa, A. Liubinas, M. Duke, Inter-layer free cobalt-doped silica membranes for pervaporation of ammonia solutions, J. Membr. Sci. 553 (2018) 111–116.
[15] T.A.C. Oliveira, U. Cocchini, J.T. Scarpello, A.G. Livingston, Pervaporation mass transfer with liquid flow in the transition regime, J. Membr. Sci. 183 (2001) 119–133.
[16] N. van Linden, H. Spanjers, J.B. van Lier, Fuelling a solid oxide fuel cell with ammonia recovered from water by vacuum membrane stripping, Chem. Eng. J. (2021) 131081.
[17] H.M. van Veen, M.D.A. Rietkerk, D.P. Shanahan, M.M.A. van Tuel, R. Kreiter, H. L. Castricum, J.E. ten Elshof, J.F. Vente, Pushing membrane stability boundaries with HybSi® pervaporation membranes, J. Membr. Sci. 380 (2011) 124–131.
[18] S. Bandini, C. Gostoli, G.C. Sarti, Separation efficiency in vacuum membrane distillation, J. Membr. Sci. 73 (1992) 217–229.
[19] K.W. Lawson, D.R. Lloyd, Membrane distillation, J. Membr. Sci. 124 (1997) 1–25.
[20] C.-K. Chiam, R. Sarbatly, Vacuum membrane distillation processes for aqueous solution treatment—a review, Chem. Eng. Process 74 (2013) 27–54.
[21] L. Martínez-Díez, M.I. Vázquez-González, Temperature and concentration polarization in membrane distillation of aqueous salt solutions, J. Membr. Sci. 156 (1999) 265–273.
[22] J.G. Wijmans, A.L. Athayde, R. Daniels, J.H. Ly, H.D. Kamaruddin, I. Pinnau, The role of boundary layers in the removal of volatile organic compounds from water by pervaporation, J. Membr. Sci. 109 (1996) 135–146.
[23] M. Khayet, T. Matsuura, Pervaporation and vacuum membrane distillation processes: modeling and experiments, AIChE J. 50 (2004) 1697–1712.
[24] S.M. Mojab, A. Pollard, J.G. Pharoah, S.B. Beale, E.S. Hanff, Unsteady laminar to turbulent flow in a spacer-filled channel, Flow, Turbul. Combust. 92 (2014) 563–577.
[25] G. Schock, A. Miquel, Mass transfer and pressure loss in spiral wound modules, Desalination 64 (1987) 339–352.
[26] N. van Linden, H. Spanjers, J.B. van Lier, Application of Dynamic Current Density for Increased Concentration Factors and Reduced Energy Consumption for Concentrating Ammonium by Electrodialysis, Water Res., 2019, p. 114856.
[27] N. van Linden, G.L. Bandinu, D.A. Vermaas, H. Spanjers, J.B. van Lier, Bipolar membrane electrodialysis for energetically competitive ammonium removal and dissolved ammonia production, J. Clean. Prod. (2020) 120788.
[28] D.R. Lide, W.M. Haynes, CRC Handbook of Chemistry and Physics : a Ready-Reference Book of Chemical and Physical Data, CRC Press, Boca Raton, Fla, 2011.